Antiepileptic drugs induce subcritical dynamics in human cortical networks

Christian Meisel[a,b,1]

[a]Department of Neurology, University Clinic Carl Gustav Carus, 01307 Dresden, Germany; and [b]Department of Neurology, Boston Children's Hospital, Boston, MA 02115

Edited by Terrence J. Sejnowski, Salk Institute for Biological Studies, La Jolla, CA, and approved March 26, 2020 (received for review July 5, 2019)

Cortical network functioning critically depends on finely tuned interactions to afford neuronal activity propagation over long distances while avoiding runaway excitation. This importance is highlighted by the pathological consequences and impaired performance resulting from aberrant network excitability in psychiatric and neurological diseases, such as epilepsy. Theory and experiment suggest that the control of activity propagation by network interactions can be adequately described by a branching process. This hypothesis is partially supported by strong evidence for balanced spatiotemporal dynamics observed in the cerebral cortex; however, evidence of a causal relationship between network interactions and cortex activity, as predicted by a branching process, is missing in humans. Here this cause–effect relationship is tested by monitoring cortex activity under systematic pharmacological reduction of cortical network interactions with antiepileptic drugs. This study reports that cortical activity cascades, presented by the propagating patterns of epileptic spikes, as well as temporal correlations decline precisely as predicted for a branching process. The results provide a missing link to the branching process theory of cortical network function with implications for understanding the foundations of cortical excitability and its monitoring in conditions like epilepsy.

cortex activity | epilepsy | branching process | criticality | antiepileptic drug

Understanding the organization of complex structural brain networks and how these structures shape dynamics is widely considered an essential step to grasp cortical network function (1–3). Cortical network functioning critically depends on a finely tuned level of excitability, the transient or steady-state response in which the brain reacts to a stimulus. Whereas small, local responses indicate a comparably small excitability, large and global responses suggest excitability in brain tissue to be high. In cortical networks, excitability must be small enough to prevent explosive growth of neuronal activity cascades on one hand. On the other hand, it must be large enough to allow for activity propagation over long distances to afford neuronal communication across sites far apart. The importance of finely tuned cortical excitability levels is highlighted by the pathological consequences and impairments resulting from aberrant network excitability in neurological (4) and psychiatric diseases (5). In epilepsy, changes in cortical network excitability are believed to be an important cause underlying the initiation and spread of seizures, i.e., the large nonphysiological neuronal activity cascades across time and space (6–8). Pharmacological reduction of excitability consequently constitutes the main treatment approach to control seizures (9).

In the brain, excitability is a product of excitatory and inhibitory network interactions. To avoid regimes where excitability is too high or too low, these interactions must be finely tuned. A growing amount of evidence indicates that this control of activity propagation by network interactions can be adequately described by a branching process (10–17). In a branching process, activity will remain small and local when interactions are too weak. When interactions are too strong, dynamics overactivates the whole network. At the critical transition between these two states, activity propagates in balanced cascades, or avalanches, avoiding premature die-out and runaway excitation. These balanced propagation patterns closely match empirical observations in animal and human studies where spontaneous activity was found to propagate from one active group of neurons to another in cascades over long distances without runaway excitation (12, 18–20). Further evidence comes from observations of long-range temporal correlations in cortical activity (16, 18, 21), another hallmark of a critical branching process (16, 17, 22). When network interactions in a branching process are reduced, cascade sizes and temporal correlations decline (10–12, 16, 17, 23). In vitro studies using cortex preparations, where network interactions can be pharmacologically reduced, show that activity changes closely match the predictions of a branching process (12). Pharmacological manipulation of network interactions was also shown to impact initiation, propagation, and termination of epileptiform activity in cortical slices from rodents (24).

Empirical evidence, however, that alterations in cortical network interactions predict dynamics changes according to a branching process in humans is missing. The lack of this cause–effect demonstration constitutes a missing link to the branching process theory with implications for understanding the foundations of cortical excitability and its management in conditions like epilepsy.

Here the hypothesis that cortical network interactions control dynamics according to a branching process in humans is directly tested. The study makes use of the notion that antiepileptic drugs (AEDs) are specifically targeted at reducing network interactions either by reduction of a neuron's individual

Significance

Activity propagation in cortex must be carefully balanced to prevent premature die-out and runaway excitation. In this study, large-scale human electrophysiology data and systematic pharmacological control of cortical network interactions are used to provide evidence that cortical network dynamics is controlled by network interactions according to a branching process. The results provide a missing link to the branching process theory of cortical network function with implications for understanding the foundations of cortical excitability, its monitoring in conditions like epilepsy, and how the balance of excitation and inhibition shapes the capacity of temporal information integration in cortical networks.

Author contributions: C.M. designed research, performed research, contributed new reagents/analytic tools, analyzed data, and wrote the paper.

The author declares no competing interests.

This article is a PNAS Direct Submission.

[1]Email: christian@meisel.de.

This article contains supporting information online at https://www.pnas.org/lookup/suppl/doi:10.1073/pnas.1911461117/-/DCSupplemental.

First published May 1, 2020.

excitability, reduction of excitatory synaptic transmission, or increase in inhibitory synaptic transmission (9). By systematic investigation of the effects of AEDs on cortex dynamics alongside a companion neural network model, the study shows that changes in network interactions predict spatiotemporal cortex dynamics precisely as expected for a branching process.

Results

A parsimonious neuron network model based on a branching process was first analyzed to review how collective cortical dynamics is shaped by network interactions and AED action. Similar models have been used widely to successfully predict the dynamics of tissue from the cortex in humans, monkeys, rats, and turtles (12, 13, 15, 16, 25–29). The model is simple enough to provide insight into the mechanisms governing collective network dynamics yet entails sufficient detail to model relevant aspects of AED action on network interactions. The network consisted of probabilistic binary neurons with all-to-all connectivity, a subset of neurons (20%) being inhibitory (Fig. 1*B*). This study's model differed from previous models in that it contains means to mimic AED action to reduce excitability (9) (Fig. 1*A*): 1) a variable p_{ne} to probabilistically reduce neuron excitability, 2) a scaling parameter p_{exc} by which excitatory synaptic strengths could be downscaled, and 3) a scaling parameter p_{inh} by which inhibitory synaptic strengths could be upscaled. How the model dynamics in terms of cascading activity and temporal correlations change as a result of decreasing excitability by means of AED action was studied.

In the absence of AED action (i.e., p_{ne}, p_{exc}, and p_{inh} all set to 1), collective dynamics exhibited the well-known phase transition from low (albeit not completely ceasing; ref. 15) activity to a high-activity phase when connection strength was increased (Fig. 1*C*, black line). Activity propagated in the form of cascades or avalanches (12, 25, 27). Cascade sizes, quantified by the large cascade fraction (LCF), became larger as interaction strength was increased, whereas temporal correlations, quantified by the autocorrelation half-width (ACW), peaked at criticality (16, 17, 21) (Fig. 1*C*, gray dashed and solid lines, respectively). Next, the effect of AED action on network state in general and on these dynamical signatures in particular was studied. The dynamics of excitable networks, such as the network model studied here, are generally characterized by the largest eigenvalue λ of the network adjacency matrix, with criticality occurring at $\lambda = 1$ (15, 27, 30, 31). AED action effectively reduced the average connectivity of the network and thus the largest eigenvalue λ of the network's adjacency matrix (Fig. S3*B*). If networks were instantiated at criticality ($\lambda = 1$) or in a slightly subcritical regime, AED action thus drove the system further into the subcritical regime ($\lambda < 1$; Fig. S3*C*). By consequence, LCF and ACW decreased with each AED mechanism of action modeled when dynamics was placed at criticality or in the subcritical regime (Fig. 1 *D* and *E*). Collectively, these model results illustrate that AED action controls network dynamics by acting on the system's control parameter, i.e., network interactions. By changing network interactions in experiment, AEDs may therefore allow to directly test if network interactions control spatiotemporal cortex dynamics as predicted by a branching process in humans.

To study cascading network events in human cortex, this study took advantage of the fact that interictal epileptic spikes superimpose in the extracellular field as a consequence of synchronous activity of spatially neighbored groups of neurons (Fig. 2*A*). Epileptic spikes consist of elevated population activity known to propagate across cortex (32). Interspike intervals exhibited a bimodal density distribution (Fig. 2*B*) indicative of short intervals arising from spikes in the same cascade and long intervals separating different cascades. Spatiotemporal spike cascades were consequently identified if spikes occurred within the same or consecutive time bins of width ΔT (Fig. 2*C*), where ΔT was chosen to be greater than the short timescale of interspike intervals within a cascade but less than the longer timescale of intercascade quiescent periods (33). Spikes were observed to organize in cascades of continuous events in time and space indicative of the presence of significant correlations in neuronal activity among cortical sites which, accordingly, were destroyed when the times of spikes were shuffled randomly (Fig. 2*D*). Cascade sizes exhibited a high degree of variability with larger sizes occurring systematically less often, as predicted by a branching process in the vicinity of criticality or in a slightly subcritical state (10–12, 14, 17). In further agreement with a branching process, cascade size distributions and the respective scaling regimes were bounded by the system size (34), which in this case corresponded to the number of electrocorticogram (ECoG) channels in each patient. Cascade size distributions sometimes exhibited the impression of a slight bump or kink in its tail but in the majority of patients did not show a pronounced or coherent indication of more than one slope (Fig. 2*D*, red), in line with modeling results. Across patients, higher AED loads were generally associated with a marked reduction in large cascade sizes (Fig. 2*D*, blue). As a quantification, the LCF was significantly lower in days with high compared to low AED load (Fig. 2*E*; $P = 0.006$, two-sided paired t test). This effect could not be explained by spike rate changes, which exhibited no difference ($P = 0.577$, two-sided paired t test; Fig. S2*A*). Note that AED intake was not always completely ceased in patients, which is why cascade size distributions were compared relative to high vs. low AED medication regimes and which may be one explanation why not all patients exhibited a perfect power-law scaling of cascade size distributions even during low AED medication days.

While the decline in large cascades under AED action visually matched the observations in the neuron network model closely (Fig. 1*D*), a more quantitative comparison between model and experiment can be challenging (35), in particular since it requires a more precise, quantitative knowledge of AED action in real-life conditions. The knowledge of how, quantitatively, an AED exerts its actions in real-life conditions is limited by the fact that the action of AEDs at the molecular level is not fully understood; the fact that most AEDs have more than one mechanism of action; the fact that concentration of a drug in the brain is not precisely known; and the fact that action depends further on metabolization rates, drug interaction, and more (9, 36, 37). Experiments using cell cultures may, however, provide some approximate estimates. Diazepam, a common AED acting on the GABA-ergic pathway, for example, has been observed to augment conductance levels in a concentration-dependent way, from approximately 50 pS at baseline to a maximum conductance of 70 to 80 pS (38). Thus, while many additional factors are clearly at play in real-life conditions, if one considered a 50% increase in inhibitory efficacy in the study's model as a biology-inspired approximate estimate, then the relative changes observed in the model were of similar order of magnitude in comparison to experimental observations (Fig. S1 *B*, *Top*).

Next, it was tested whether temporal correlations were controlled by AEDs as predicted by a branching process. Modulations in signal power are a generally useful currency in characterizing neural dynamics (39). The study analyzed broadband high-frequency power modulations which provide a local estimate of population spike rate variations near an electrocorticographic electrode (40–44). Autocorrelation functions obtained from these high-frequency power modulation have been shown to accurately capture temporal integration properties (45). Autocorrelation functions exhibited a faster decay in high AED medication days compared to low medication days (Fig. 3*A*). As a quantification of this decay, the ACW was significantly lower in days with high compared to low AED load (Fig. 3*B*;

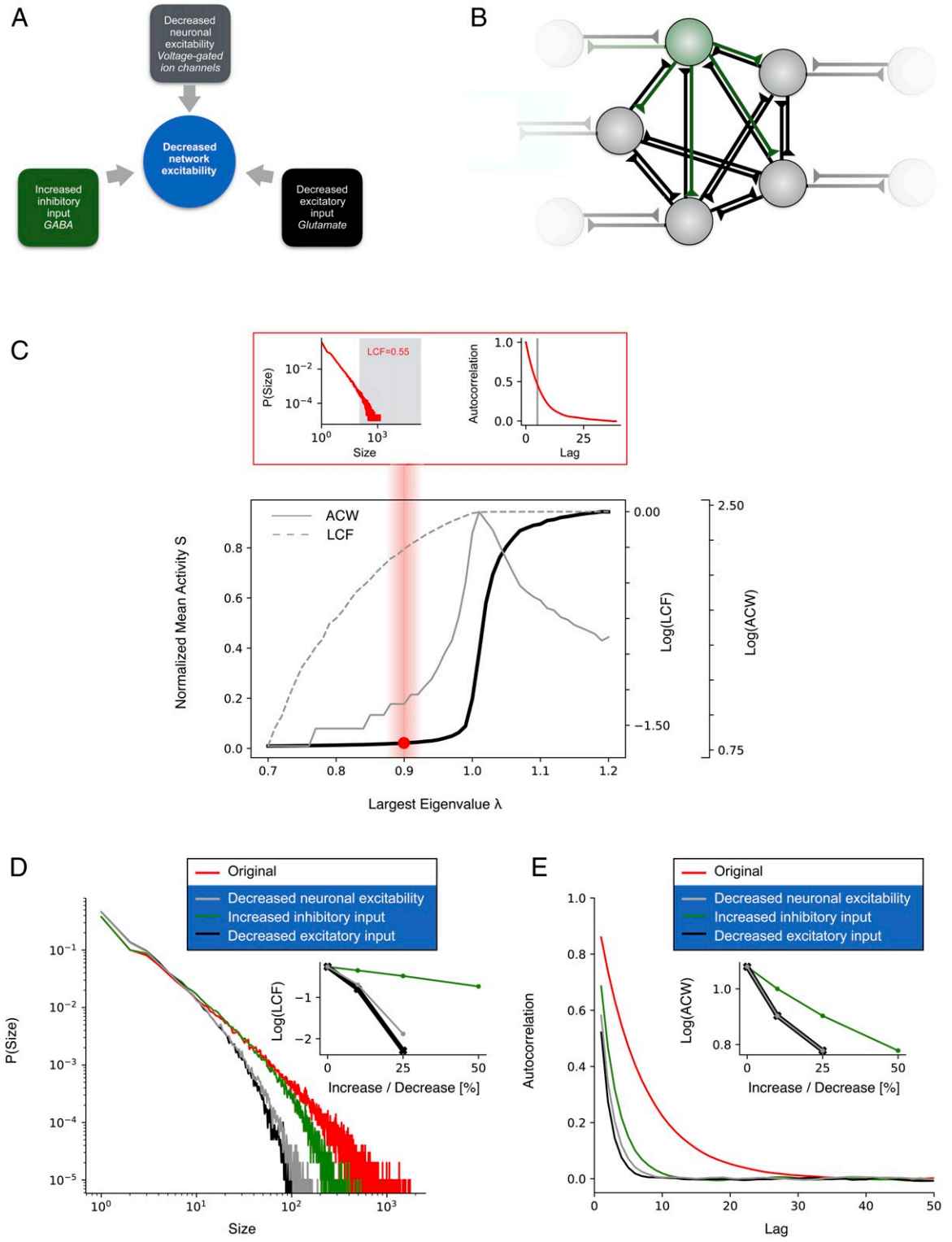

Fig. 1. AED action induces subcritical dynamics in a neural network model. (*A*) Illustration of the main mechanisms of AED action. Collectively, AEDs are designed to reduce seizure risk by decreasing cortical network excitability. (*B*) Conceptual cartoon illustrating neural network model features, including excitatory (black) and inhibitory (green) recurrent synapses. The strengths of inhibitory and excitatory synaptic transmission along with individual neuron excitability can be selectively changed to mimic AED action. (*C*) Network dynamics exhibits a phase transition between an inactive phase, where cascades remain small and local, and an active phase, where activity is dominated by large cascades spanning the whole network upon increasing connection strengths (solid black line). Gray dashed line indicates the LCF. Gray solid line indicates ACW, which peaks at criticality ($\lambda = 1$). Red box shows cascade size distribution and autocorrelation functions when dynamics is poised in a slightly subcritical regime, mimicking experimental observations under low AED load. (*D* and *E*) AED action incurs decline of large cascade sizes and faster autocorrelation function decay. Large plots show exemplary cascade size distribution and autocorrelation function (25% decrease in neuron excitability, 25% decrease in excitatory synaptic strength, and 50% increase in inhibitory synaptic strength). (*Insets*) LCF and ACW for a range of network excitability reducing parameter values.

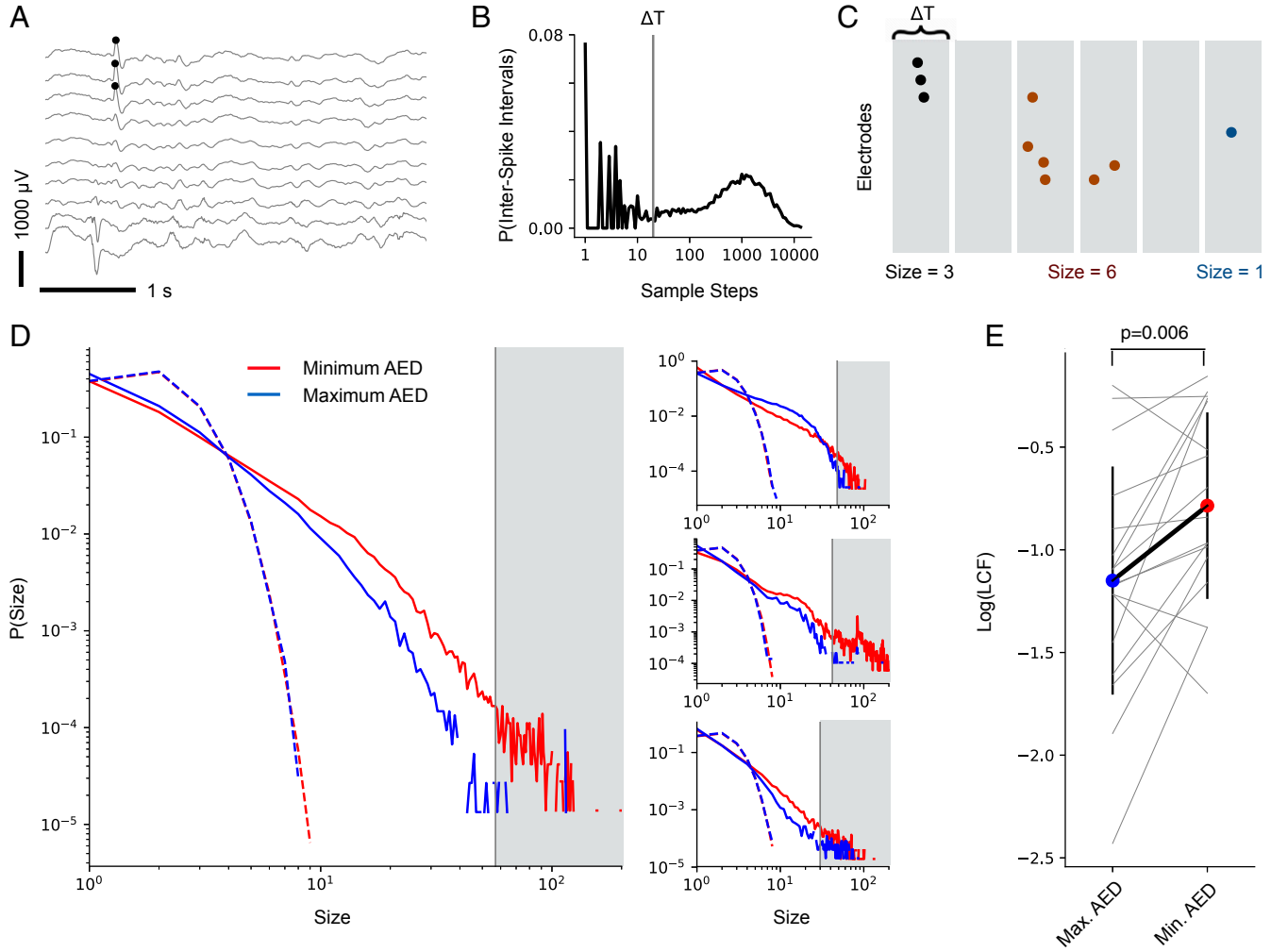

Fig. 2. Epileptic spikes organize as activity cascades reduced in size by AED action. (*A*) Identification of spikes in electrocorticogram. (*B* and *C*) Bimodality of interspike interval distribution identifies spike cascades and their timescale. (*D*) Spike cascade size distribution from four patients during high (blue) and low (red) AED load days. High AED load reduces the number of large cascades (shaded gray area). Broken lines indicate size distributions from randomly shuffled spike times. (*E*) AEDs significantly reduce the number of large cascades (gray lines indicate individual patients; black line indicates mean with whiskers denoting SD).

$P = 0.007$, two-sided paired t test). This effect could not be explained by changes in high-frequency power, which exhibited no difference ($P = 0.988$, two-sided paired t test). The relative changes observed in the model were again qualitatively comparable to the experimental data when biology-inspired estimates of AED action (38) were incorporated in the model (Fig. S1 *B*, *Bottom*). Again, an exact quantitative comparison between model and experiment is limited by the facts that the action of AEDs at the molecular level is not fully understood; that most AEDs have more than one mechanism of action; that drug concentrations in the brain are not precisely known; and that action depends further on metabolization rates, drug interaction, and more (9, 36, 37). Thus, the larger autocorrelation change observed in the model in comparison to data (Fig. S1 *B*, *Bottom*) may relate to the fact that the changes in cascade size are also more limited in the data than in the model (Fig. S1 *B*, *Top*) and, collectively, may suggest that diazepam, under in vivo conditions, potentially leads to a smaller increase in inhibitory efficacy than what is observed under in vitro conditions (38).

The changes in cascade sizes and temporal correlations occurred despite no relevant change in spike rate or signal power in the ECoG data. It is important to consider that rate changes can, in principle, give the impression of altered cascade size distributions (46) or, under high levels of external forcing or spontaneous network activity, can lead to a lack of critical dynamics altogether (47). To further explore cascade sizes and temporal correlations under rate-matched conditions, the study revisited the model and matched the model's spike (or event) rate to the one observed experimentally (Fig. S2*A*). Under these rate-matched conditions, model cascade sizes and temporal correlations similarly declined under AED action and closely mimicked experimental observations (Fig. S2*B*). Collectively, the close match between model and experiments thus provides strong indication that the observed changes are not simply an effect of event rate (46, 47) but due to an underlying network state change with a shift toward subcritical dynamics.

Discussion

The results demonstrate that human cortical dynamics under manipulation of network interactions by AEDs is predicted by a branching process. Albeit backed by a large number of computational studies (16, 23, 25–29, 48, 49), empirical evidence demonstrating interaction strength as a control parameter in this phase space had previously been limited to reduced in vitro

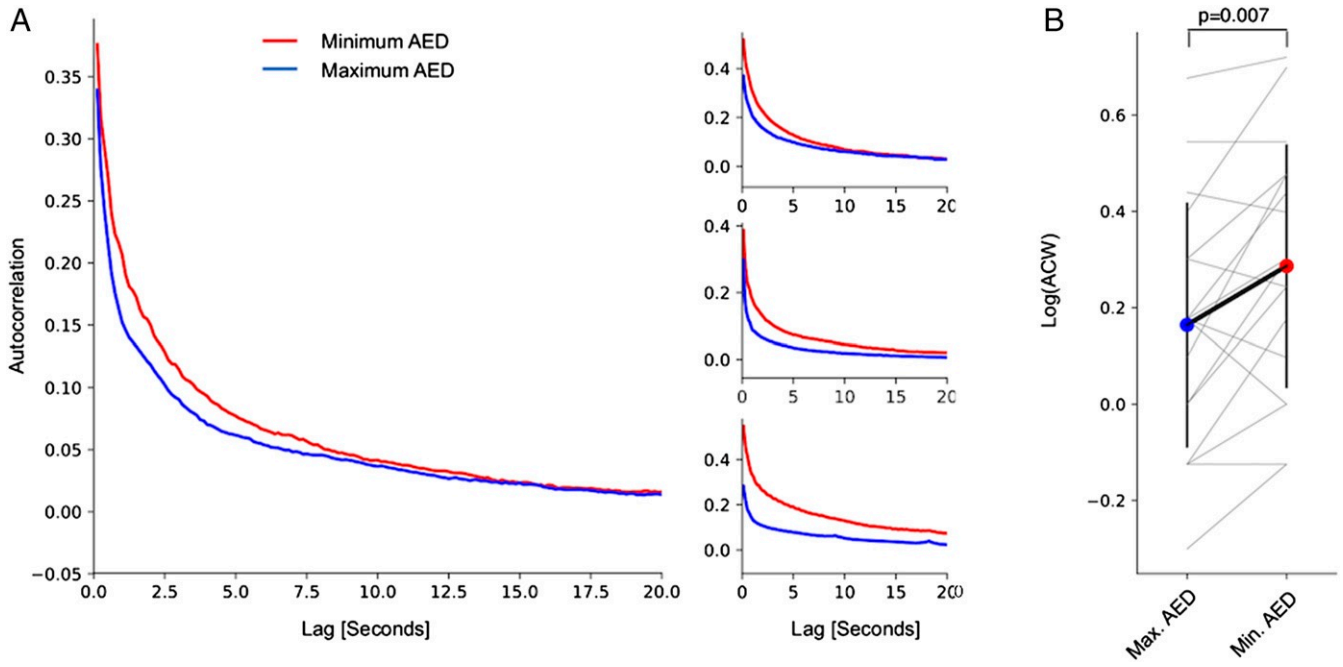

Fig. 3. AED action reduces temporal correlations in cortex. (*A*) Autocorrelation functions from four patients during high (blue) and low (red) AED load days. (*B*) AEDs significantly reduce temporal correlations measured by the autocorrelation function half-width (ACW; gray lines indicate individual patients; black line indicates mean with whiskers denoting SD).

preparations (12). A growing number of empirical and theoretical studies suggest that human cortical network dynamics is normally poised at criticality or in a slightly subcritical regime (18, 21, 47, 49–54). By using AEDs as means to pharmacologically manipulate and reduce cortical network interactions in epilepsy patients, the study reports that dynamics becomes more short ranged in terms of spatiotemporal activity cascades and temporal correlations. These findings closely match predictions for dynamical shifts toward the subcritical state, as demonstrated in a companion model. By directly controlling network interaction in patients, this work overcomes previous limitations inherent to passive monitoring of network dynamics. Note that AED intake was not always completely ceased in patients, which may be one explanation why not all patients exhibited a perfect power-law scaling of cascade size distributions even during low AED medication days. Another potential explanation for why not all patients exhibited a perfect power-law scaling even during low AED medication days may be related to some research suggesting that realistic neural networks always show some slightly subcritical behavior due to the level of spontaneous activity occurring in those networks (47). However, regardless of whether dynamics is normally critical or slightly subcritical, the results indicate that AEDs drive cortical network dynamics further into a subcritical regime by acting on the control parameter, which may serve to avoid the risk of runaway excitation (Fig. 4).

This work adds to a rapidly growing amount of research on the relevance of phase transitions and bifurcations in normal, healthy cortex dynamics and in diseases like epilepsy. The concept of phase transitions stems traditionally from physics, and bifurcations constitute their mathematical analogs. Bifurcations have been shown to underlie the offset of epileptic seizures (55); the role of bifurcations at seizure onset is currently the topic of ongoing discussions (56–58). The idea that a bifurcation or phase transition point is crossed at seizure onset may be supported by observations of a breakdown of the scale-free dynamics characterizing normal cortex dynamics during epileptic seizures (51). However, whether this transition point corresponds to a critical transition associated with a branching process or to some other bifurcation demands further research. Overall, the hope is that by advancing insights into the underlying mechanisms of seizure onset and offset as well as insights into the determinants of normal cortical functioning, bifurcation or phase transition theory may lead to a better understanding of normal cortex dynamics and ictogenesis and better translation into methods for the

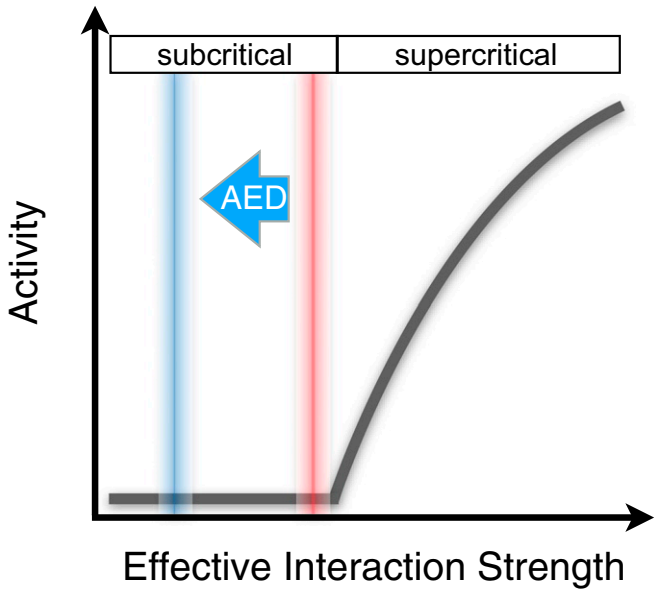

Fig. 4. Growing evidence suggests that activity propagation in cortical networks can be described by a branching process near the transition between an inactive (subcritical) and an active (supercritical) phase (red). AEDs shift network dynamics farther into the subcritical phase (blue), thereby establishing a safety margin to avoid runaway activity associated with the supercritical phase.

detection, prediction, and control of seizures and will eventually, based on better diagnostics, afford improved treatments (59).

In order to understand brain function, understanding the organization of complex structural brain networks and how structure shapes dynamics on these networks is an essential step (1–3). One of the central concepts of brain network science is effective connectivity, which attempts to capture a network of directed causal effects between neural elements (60, 61). While concepts like effective connectivity are widely used, they are best tested by direct perturbation, and in humans, pharmacological manipulation might be one of few feasible ways to do this. The decrease in activity spread across cortical networks observed in this study's data under systematic reduction of network interactions is well aligned with expectations for reduced effective connectivity (60, 61). A branching process can be considered a more specific extension of the effective connectivity framework by adding a precise quantitative component that dictates how specifically, i.e., quantitatively, spatiotemporal dynamics changes as a function of network interactions. The confirmation of quantitative predictions from a branching process in cortex (16, 23, 25–29, 48, 49) in this work can thus also be considered a validation of the more qualitative effective connectivity concept.

Beyond providing a missing link to the branching process theory of cortical network function, the current findings have implications for understanding the foundations of cortical excitability and information processing in cortex. Aberrant excitability levels are an important cause underlying the initiation and spread of seizures (6–8). Accordingly, the ability to monitor excitability and control its degree is of prime importance for adequate clinical care and treatment. As a unifying framework linking interictal spike cascades, temporal correlations, and cortical network excitability, a branching process provides precise markers informed by theory on how to monitor excitability levels from EEG (62). For example, while previous work has shown that interictal spike count itself does not reflect excitability (63), a branching process, backed by this study's empirical findings, suggests that cascade sizes of interictal spikes are more informative about network excitability. The diminished spread of neural activity to other cortical sites indicated by the smaller cascades under high AED load is in line with observations of lower synchrony under AEDs (62) indicative of decreased cortical interactions. Collectively, a fundamental dynamical understanding of how excitability and its control represents in cortical activity may help to screen and evaluate treatments targeted at excitability in epilepsy and beyond.

The study here monitored activity spread across cortex using epileptic spikes. Motivated by predictions from a branching process, it was observed that the size distribution of epileptic spike cascades was informative about AED action, whereas simple spike rate was not. These observations may help to resolve some at times controversial findings with regard to the meaning of epileptic spikes as a marker of cortical excitability, seizure propensity, and how spikes are impacted by AEDs (64). While several studies have suggested that spike rate, and, more generally, interictal epileptiform discharges, are reduced by AEDs (65), other studies have questioned their relationship to seizure likelihood and excitability by reporting no (66) or even positive relationships between spike rate and AED load (67). A recent study using long-term intracranial data concluded that the relationship between epileptic spike rates and seizures was subject-specific (68), which adds further to the notion that spike rate may not be a robust marker of AED action and cortical excitability levels. The branching process framework may help to reconcile these findings by suggesting that the spike cascade size distribution, not spike rate, is a more appropriate metric capturing AED action and its effect on cortical excitability levels in a predictable way. While spike rates may change without an underlying change in network excitability, for example, due to varying levels of external drive, the cascade size distribution remains a marker of the underlying dynamical state, if these rate changes are accounted for in the analysis (46). Monitoring of spike cascades instead of spike rates may thus help to resolve some of these long-standing controversies on spikes and their relationship to AED action, cortical excitability, and seizure propensity (64).

The maintenance and integration of information over extended periods of time is considered to be important for information processing at the neural network level (69, 70) for which long-range temporal correlations are thought to provide the neural basis (16, 45, 71, 72). Consequently, theory and experiment show that a balanced state, where long-range temporal correlation peak, gives rise to optimal information processing (13, 18, 25, 33). This study's results demonstrate a systematic decrease in temporal correlations with AED load, some of which are known to have detrimental effects on cognition. The insights gained into the decline of spatiotemporal correlation as a function of decreased cortical excitability may thus help to uncover the underlying neuronal correlates linked to these cognitive impairments.

Materials and Methods

Preprocessing of Electrocorticogram Data. Multiday electrocorticogram recordings from 17 patients undergoing presurgical monitoring at the Epilepsy Center of the University Hospital of Freiburg, Germany, were analyzed. The study was approved by the ethics committee of the University of Freiburg, and all subjects had signed informed consent that their clinical data might be used and published for research purposes. The number and dosing level of AEDs varied over the course of the recording period. The number of electrodes varied between patients and included both surface and depth electrodes (mean number of electrodes $n = 78 \pm 24$, 30 to 121). Electrode placement was solely determined by clinical considerations. Electrocorticogram data were sampled at either 256, 512, or 1,024 Hz. If sampled at higher rate, data were first downsampled to 256 Hz. A notch filter was then applied to remove potential contamination with 50 Hz line noise. Data were preprocessed in segments of 1 h duration. To compare high and low AED medication regimes, the day with the highest cumulative AED load and the day with the lowest AED load in each patient were picked and all hours from midnight to midnight within this day were analyzed. If there was more than 1 d with highest and/or lowest medications, the study picked the 2 d farthest apart from each other.

Detection of Epileptic Spikes. Spikes are large, abnormal discharges that occur between seizures in patients with epilepsy. Sharply contoured waveforms as spikes via a previously validated method (Fig. 2*A* and ref. 73) were detected here. In brief, for each 1-min-long data block, potential spikes were detected, if they crossed a threshold defined by standard deviations (SD coefficient = 4) of the absolute amplitude of high bandpass filtered signal (20 to 50 Hz, second-order digital Butterworth filter) for the channel. Next, the raw ECoG data were bandpass filtered between 1 and 35 Hz (second-order digital Butterworth filter), and all channels in the 1-min block were scaled by a scaling factor which is the median value of the average absolute amplitudes across all channels in the patient. Once data had been scaled, shape criteria of amplitude, duration, and slope were applied to the scaled, lower bandpass filtered EEG signal (1 to 35 Hz) at the previously identified potential spikes. Spike duration was determined by searching 10 sampling steps (at 256 Hz) on either side of the detected peak to find the minima on each side. Standard parameters described previously were used to identify spikes (73): total amplitude of both half-waves > 600 μV, slope of each half-wave > 7 μV/ms, and duration of each half-wave > 10 ms. Timestamps of spike maxima were saved for further analysis.

Detection of Spike Cascades. Fig. 2*B* shows the distribution of interspike intervals from one patient. The bimodality indicates a short timescale belonging to the interspike intervals within a cascade (left peak), and a much longer timescale indicative of the intervals between cascades (right peak). A cascade was defined as a spatiotemporal cluster of consecutive spikes with interspike intervals not exceeding a temporal threshold ΔT. ΔT was chosen to be in the trough between the two peaks ($\Delta T = 20$ sampling steps at 256 Hz sampling; gray vertical line in Fig. 2*B*) in order to identify

spikes belonging to one cascade and to prevent concatenation of separate cascades.

At criticality, cascade size distributions follow a power-law distribution bounded by the system size (34), whereas subcritical/supercritical dynamics are characterized by a decreased/increased incidence of larger cascades (12). Here, cascades were defined as large, if their size was greater than half the system size, i.e., half the number of channels. To quantify the relative incidence of large cascades, the large cascade fraction, LCF, was defined as the ratio between the sum of all large cascades sizes (i.e., cascades with size greater than half the system size) and the sum of all cascades sizes.

Signal Autocorrelation. Modulations in signal power are generally useful to characterize neural dynamics (39). In particular, fluctuations in the broadband high-frequency 50 to 200 Hz range have been shown to provide a local, spatiotemporal estimate of population spike rate variations near an electrode (40–44).

For each ECoG channel, time courses of broadband high-frequency power fluctuations were obtained by computing the mean 50 to 100 Hz signal power every 125 ms (fast Fourier transform [FFT] routine, Hanning window) for each hour during either a high or low AED medication day. Signal power estimates are not normally distributed across time samples; the logarithm of power estimates was thus first taken to normalize these time series data (45, 74). Next, an autocorrelation function of these normalized power time series was obtained for each electrode and hour in recording. Analyses in the main part of the manuscript are based on average autocorrelation functions across all electrodes and across all hours in either high or low AED medication day for each patient.

ACW was defined as the full width at half maximum of the autocorrelation function of the power time course. ACW was determined as twice the time lag at which the ACF became smaller than half its value between maximum to minimum. Since time lags are in 125-ms increments, the minimal value of ACW is 0.25 s.

Computational Neuron Network Model. The neuron network model consists of $N = 200$ binary-state neurons connected by all-to-all, asymmetric synaptic coupling strengths w_{ij}. Each neuron j is either excitatory or inhibitory, corresponding to $w_{ij} \geq 0$ or $w_{ij} \leq 0$, respectively, for all i. The binary state $s_i(t+1)$ of neuron i ($s = 0$ inactive, $s = 1$ spiking) is determined based on the sum $p(t+1)$ of its inputs $p(t+1) = \sum_{j=1}^{N} w_{ij}(t)s_j(t)$ and the parameter controlling neuronal excitability, p_{ne}, according to the following dynamical rules: if $0 < p < 1$, then the neuron fires with probability $p * p_{ne}$; if $p \geq 1$, then the neuron fires with probability p_{ne}; and if $p \leq 0$, then the neuron does not fire. Note that p_{ne} applies to both inhibitory and excitatory neurons.

The dynamics of excitable networks are generally characterized by the largest eigenvalue λ of the network adjacency matrix w_{ij}, with criticality occurring at $\lambda = 1$ (15, 27, 30, 31). At $\lambda < 1$, activity is low (albeit may not cease completely; ref. 15) and does not excite the whole network, and the system is subcritical. At $\lambda > 1$, each neuron excites, on average, more than one postsynaptic neuron, and the system is supercritical. An appropriate order parameter is the aggregate activity of the network, defined as $S(t) = N^{-1} \sum_i s_i(t)$, the fraction of nodes that are excited at time t (15). Fig. 1*C*, black line, shows the normalized mean activity S, i.e., $S(t)$ averaged over time. In order to construct networks with a particular λ, w_{ij} values are first drawn from a uniform distribution [0,1]. Then, 20% of neurons are set to being inhibitory (by multiplication of the corresponding coupling strengths with –1) and the remaining 80% of neurons to being excitatory. w_{ij} are then multiplied by $N \cdot K / \sum w_{ij}$ (27, 29), where K, a measure of the average connection strength, is closely related to the desired λ (Fig. S3*A*).

The model affords implementation of different AED mechanisms known to reduce cortical network excitability: reduction of individual neuronal excitability, reduction of excitatory synaptic transmission, and increase of inhibitory synaptic transmission (Fig. 1*A* and ref. 9). Reduction of individual neuronal excitability is controlled by parameter p_{ne}, where $p_{ne} \leq 1$. Decreased excitatory synaptic transmission is modeled by multiplication of all positive w_{ij} with factor p_{exc}, where $p_{exc} \leq 1$. Increased inhibitory synaptic transmission is modeled by multiplication of all negative w_{ij} with factor p_{inh}, where $p_{inh} \geq 1$.

The onset of stimulation is instantiated by setting a random neuron to active. Activity is monitored until 500 time steps have passed or until activity has died out, at which point a new cascade is started by setting a random neuron to active. A total of 100,000 such cascades at each λ and for each AED mechanism were modeled. The temporal autocorrelation was studied using the time course of overall network activity, i.e., the sum of active neurons at each time step.

The study also evaluated cascade size distribution and temporal correlations in the model under conditions where the spike (or event) rate in the model was matched to the experimentally observed spike rates. Experimentally, a constant spike rate of approximately two spikes per minute and ECoG channel under high and low AED load was observed (Fig. S2*A*). Experimental interspike intervals exhibited a bimodal density distribution (Fig. 2*B*) indicative of an effective timescale separation analogous to this study's model: a short timescale corresponding to the intervals arising from spikes in the same cascade and a long timescale corresponding to the intervals separating different cascades. Consequently, an experimentally observed spike rate of two spikes per minute (Fig. S2*A*) monitored over 24 h corresponded to 576,000 spikes (or events) in this study's model with 200 channels (2 spikes per min per channel $\times$ 200 channels $\times$ 1,440 min). The study therefore analyzed cascade size distributions and temporal correlations for exactly 576,000 spikes in each condition in the study's model to match the experimental event rate and data over 24 h. Under these rate-matched conditions to experiment, model cascade sizes and temporal correlations continued to decline under AED action and closely mimicked experimental observations (Fig. S2*B*).

Data Availability Statement. All patient data are available from a data repository (75), and custom code used for analysis is available from the author upon reasonable request.

1. O. Sporns, *Networks of the Brain* (MIT Press, Cambridge, MA, 2010).
2. K. J. Friston, Modalities, modes, and models in functional neuroimaging. *Science* **326**, 399–403 (2009).
3. D. S. Bassett, O. Sporns, Network neuroscience. *Nat. Neurosci.* **20**, 353–364 (2017).
4. R. A. Badawy, T. Loetscher, R. A. Macdonell, A. Brodtmann, Cortical excitability and neurology: Insights into the pathophysiology. *Funct. Neurol.* **27**, 131–145 (2012).
5. F. Masuda *et al.*, Motor cortex excitability and inhibitory imbalance in autism spectrum disorder assessed with transcranial magnetic stimulation: A systematic review. *Transl. Psychiatry* **9**, 110 (2019).
6. C. E. Stafstrom, Epilepsy: A review of selected clinical syndromes and advances in basic science. *J. Cereb. Blood Flow Metab.* **26**, 983–1004 (2006).
7. M. Bazhenov, I. Timofeev, F. Frohlich, T. J. Sejnowski, Cellular and network mechanisms of electrographic seizures. *Drug Discov. Today Dis. Models* **5**, 45–57 (2008).
8. A. J. Trevelyan, C. A. Schevon, How inhibition influences seizure propagation. *Neuropharmacology* **69**, 45–54 (2013).
9. M. Bialer, H. S. White, Key factors in the discovery and development of new antiepileptic drugs. *Nat. Rev. Drug Discov.* **9**, 68–82 (2010).
10. T. E. Harris, *The Theory of Branching Processes* (Dover Publications, New York, 1989).
11. S. Zapperi, K. Baekgaard Lauritsen, H. Stanley, Self-organized branching processes: Mean-field theory for avalanches. *Phys. Rev. Lett.* **75**, 4071–4074 (1995).
12. J. M. Beggs, D. Plenz, Neuronal avalanches in neocortical circuits. *J. Neurosci.* **23**, 11167–11177 (2003).
13. C. Haldeman, J. Beggs, Critical branching captures activity in living neural networks and maximizes the number of metastable states. *Phys. Rev. Lett.* **94**:058101 (2005).
14. D. Plenz, Neuronal avalanches and coherence potentials. *Eur. Phys. J.* **205**, 259–301 (2012).
15. D. B. Larremore, W. L. Shew, E. Ott, F. Sorrentino, J. G. Restrepo, Inhibition causes ceaseless dynamics in networks of excitable nodes. *Phys. Rev. Lett.* **112**, 138103 (2014).
16. C. Meisel, A. Klaus, V. V. Vyazovskiy, D. Plenz, The interplay between long- and short-range temporal correlations shapes cortex dynamics across vigilance states. *J. Neurosci.* **37**, 10114–10124 (2017).
17. J. Wilting, V. Priesemann, Inferring collective dynamical states from widely unobserved systems. *Nat. Commun.* **9**, 2325 (2018).
18. J. M. Palva *et al.*, Neuronal long-range temporal correlations and avalanche dynamics are correlated with behavioral scaling laws. *Proc. Natl. Acad. Sci. U.S.A.* **110**, 3585–3590 (2013).
19. A. Haimovici, E. Tagliazucchi, P. Balenzuela, D. R. Chialvo, Brain organization into resting state networks emerges at criticality on a model of the human connectome. *Phys. Rev. Lett.* **110**, 178101 (2013).
20. T. Bellay, A. Klaus, S. Seshadri, D. Plenz, Irregular spiking of pyramidal neurons organizes as scale-invariant neuronal avalanches in the awake state. *Elife* **4**, e07224 (2015).
21. K. Linkenkaer-Hansen, V. V. Nikouline, J. M. Palva, R. J. Ilmoniemi, Long-range temporal correlations and scaling behavior in human brain oscillations. *J. Neurosci.* **21**, 1370–1377 (2001).
22. P. Bak, C. Tang, K. Wiesenfeld, Self-organized criticality: An explanation of the 1/f noise. *Phys. Rev. Lett.* **59**, 381–384 (1987).
23. H. Markram *et al.*, Reconstruction and simulation of neocortical microcircuitry. *Cell* **163**, 456–492 (2015).
24. D. J. Pinto, S. L. Patrick, W. C. Huang, B. W. Connors, Initiation, propagation, and termination of epileptiform activity in rodent neocortex in vitro involve distinct mechanisms. *J. Neurosci.* **25**, 8131–8140 (2005).

25. O. Kinouchi, M. Copelli, Optimal dynamical range of excitable networks at criticality. *Nat. Phys.* **2**, 348–351 (2006).
26. S. S. Poil, A. van Ooyen, K. Linkenkaer-Hansen, Avalanche dynamics of human brain oscillations: Relation to critical branching processes and temporal correlations. *Hum. Brain Mapp.* **29**, 770–777 (2008).
27. D. B. Larremore, W. L. Shew, J. G. Restrepo, Predicting criticality and dynamic range in complex networks: Effects of topology. *Phys. Rev. Lett.* **106**, 058101 (2011).
28. W. L. Shew, H. Yang, S. Yu, R. Roy, D. Plenz, Information capacity and transmission are maximized in balanced cortical networks with neuronal avalanches. *J. Neurosci.* **31**, 55–63 (2011).
29. W. L. Shew *et al.*, Adaptation to sensory input tunes visual cortex to criticality. *Nat. Phys.* **11**, 659–663 (2015).
30. S. Pei *et al.*, How to enhance the dynamic range of excitatory-inhibitory excitable networks. *Phys. Rev. E Stat. Nonlin. Soft. Matter. Phys.* **86**, 021909 (2012).
31. D. B. Larremore, M. Y. Carpenter, E. Ott, J. G. Restrepo, Statistical properties of avalanches in networks. *Phys. Rev. E Stat. Nonlin. Soft. Matter. Phys.* **85**, 066131 (2012).
32. J. M. Badier, P. Chauvel, Spatio-temporal characteristics of paroxysmal interictal events in human temporal lobe epilepsy. *J. Physiol. Paris* **89**, 255–264 (1995).
33. W. L. Shew, H. Yang, T. Petermann, R. Roy, D. Plenz, Neuronal avalanches imply maximum dynamic range in cortical networks at criticality. *J. Neurosci.* **9**, 15595–15600 (2009).
34. S. Yu, A. Klaus, H. Yang, D. Plenz, Scale-invariant neuronal avalanche dynamics and the cut-off in size distributions. *PLoS ONE* **9**, e99761 (2014).
35. A. B. Holt, T. I. Netoff, Computational modeling of epilepsy for an experimental neurologist. *Exp. Neurol.* **244**, 75–86 (2013).
36. R. L. Macdonald, K. M. Kelly, Antiepileptic drug mechanisms of action. *Epilepsia* **36**, 2–12 (1995).
37. C. J. Landmark, Targets for antiepileptic drugs in the synapse. *Med. Sci. Monit.* **13**, 1–7 (2007).
38. M. Eghbali, J. P. Curmi, B. Birnir, P. W. Gage, Hippocampal GABA(A) channel conductance increased by diazepam. *Nature* **388**, 71–75 (1997).
39. T. H. Donner, M. Siegel, A framework for local cortical oscillation patterns. *Trends Cogn. Sci. (Regul. Ed.)* **15**, 191–199 (2011).
40. J. R. Manning, J. Jacobs, I. Fried., M. J. Kahana, Broadband shifts in local field potential power spectra are correlated with single-neuron spiking in humans. *J. Neurosci.* **29**, 13613–13620 (2009).
41. K. J. Miller, Broadband spectral change: Evidence for a macroscale correlate of population firing rate?*J. Neurosci.* **30**, 6477–6479 (2010).
42. Y. Nir *et al.*, Coupling between neuronal firing rate, gamma LFP, and BOLD fMRI is related to interneuronal correlations. *Curr. Biol.* **17**, 1275–1285 (2007).
43. S. Ray, J. H. Maunsell, Different origins of gamma rhythm and high-gamma activity in macaque visual cortex. *PLoS Biol.*. **9**, e1000610 (2011).
44. K. Whittingstall, N. K. Logothetis, Frequency-band coupling in surface EEG reflects spiking activity in monkey visual cortex. *Neuron* **64**, 281–289 (2009).
45. C. J. Honey *et al.*, Slow cortical dynamics and the accumulation of information over long timescales. *Neuron* **76**, 423–434 (2012).
46. S. Yu *et al.*, Maintained avalanche dynamics during task-induced changes of neuronal activity in nonhuman primates. *Elife* **6**, e27119 (2017).
47. R. V. Williams-Garcia, M. Moore, J. M. Beggs, G. Ortiz, Quasicritical brain dynamics on a nonequilibrium Widom line. *Phys. Rev. E Stat. Nonlin .Soft. Matter Phys.* **90**, 062714 (2014).
48. C. Meisel, T. Gross, Adaptive self-organization in a realistic neural network model. *Phys. Rev. E* **80**, 061917 (2009).
49. D. R. Chialvo, Emergent complex neural dynamics. *Nat. Phys.* **6**, 744–750 (2010).
50. E. Tagliazucchi, P. Balenzuela, D. Fraiman, D. R. Chialvo, Criticality in large-scale brain FMRI dynamics unveiled by a novel point process analysis. *Front. Physiol.* **3**, 15 (2012).
51. C. Meisel, A. Storch, S. Hallmeyer-Elgner, E. Bullmore, T. Gross, Failure of adaptive self-organized criticality during epileptic seizure attacks. *PLoS Comput. Biol.* **8**, e1002312 (2012).
52. G. Deco, V. K. Jirsa, Ongoing cortical activity at rest: Criticality, multistability, and ghost attractors. *J. Neurosci.* **32**, 3366–3375 (2012).
53. C. Meisel, E. Olbrich, O. Shriki, P. Achermann, Fading signatures of critical brain dynamics during sustained wakefulness in humans. *J. Neurosci.* **33**, 17363–17372 (2013).
54. R. Chaudhuri, B. J. He, X. J. Wang, Random recurrent networks near criticality capture the broadband power distribution of human ECoG dynamics. *Cereb. Cortex* **28**, 3610–3622 (2018).
55. M. A. Kramer *et al.*, Human seizures self-terminate across spatial scales via a critical transition. *Proc. Natl. Acad. Sci. U.S.A.* **109**, 21116–21121 (2012).
56. C. Meisel, C. Kuehn, Scaling effects and spatio-temporal multilevel dynamics in epileptic seizures. *PLoS ONE* **7**, e30371 (2012).
57. V. K. Jirsa, W. C. Stacey, P. P. Quilichini, A. I. Ivanov, C. Bernard, On the nature of seizure dynamics. *Brain* **137**, 2210–2230 (2014).
58. W. C. Chang *et al.*, Loss of neuronal network resilience precedes seizures and determines the ictogenic nature of interictal synaptic perturbations. *Nat. Neurosci.* **21**, 1742–1752 (2018).
59. C. Meisel, T. Loddenkemper, Seizure prediction and intervention. *Neuropharmacology*, 10.1016/j.neuropharm.2019.107898 (2019).
60. K. J. Friston, Functional and effective connectivity: A review. *Brain Connect.* **1**, 13–36 (2011).
61. O. Sporns, Structure and function of complex brain networks. *Dialogues Clin. Neurosci.* **15**, 247–262 (2013).
62. C. Meisel *et al.*, Intrinsic excitability measures track antiepileptic drug action and uncover increasing/decreasing excitability over the wake/sleep cycle. *Proc. Natl. Acad. Sci. U.S.A.* **112**, 14694–14699 (2015).
63. W. Stacey, M. Le Van Quyen, F. Mormann, A. Schulze-Bonhage, What is the present-day EEG evidence for a preictal state?*Epilepsy Res.* **97**, 243–251 (2011).
64. B. Abou-Khalil, The ambiguous relationship between spikes and seizures. *Clin. Neurophysiol.* **127**, 3176–3177 (2016).
65. F. Buchthal, O. Svensmark, P. J. Schiller, Clinical and electroencephalographic correlations with serum levels of diphenylhydanotin. *Arch. Neurol.* **2**, 624–630 (1960).
66. J. Gotman, M. G. Marciani, Electroencephalographic spiking activity, drug levels, and seizure occurrence in epileptic patients. *Ann. Neurol.* **17**, 597–603 (1985).
67. Goncharova II *et al.*, Intracranially recorded interictal spikes: Relation to seizure onset area and effect of medication and time of day. *Clin. Neurophysiol.* **124**, 2119–2128 (2013).
68. P. J. Karoly *et al.*, Interictal spikes and epileptic seizures: Their relationship and underlying rhythmicity. *Brain* **139**, 1066–1078 (2016).
69. S. J. Kiebel, J. Daunizeau, K. J. Friston, A hierarchy of time-scales and the brain. *PLoS Comput. Biol.* **4**, e1000209 (2008).
70. K. Friston, M. Breakspear, G. Deco, Perception and self-organized instability. *Front. Comput. Neurosci.* **6**, 44 (2012).
71. R. Chaudhuri, K. Knoblauch, M. A. Gariel, H. Kennedy, X. J. Wang, A large-scale circuit mechanism for hierarchical dynamical processing in the primate cortex. *Neuron* **88**, 419–431 (2015).
72. M. L. Kringelbach, A. R. McIntosh, P. Ritter, V. K. Jirsa, G. Deco, The rediscovery of slowness: Exploring the timing of cognition. *Trends Cogn. Sci. (Regul. Ed.)* **19**, 616–628 (2015).
73. D. T. Barkmeier *et al.*, High inter-reviewer variability of spike detection on intracranial EEG addressed by an automated multi-channel algorithm. *Clin. Neurophysiol.* **123**, 1088–1095. (2012).
74. K. J. Miller, S. Zanos, E. E. Fetz, M. den Nijs, J. G. Ojemann, Decoupling the cortical power spectrum reveals real-time representation of individual finger movements in humans. *J. Neurosci.* **29**, 3132–3137 (2009).
75. M. Ihle *et al.*, EPILEPSIAE—A European epilepsy database. *Comput Methods Programs Biomed* **106**, 127–138 (2012).